

PAPER • OPEN ACCESS

## Analysis of the machine frame stiffness using numerical simulation

To cite this article: Š Vrtiel *et al* 2017 *IOP Conf. Ser.: Mater. Sci. Eng.* **266** 012015

View the [article online](#) for updates and enhancements.

You may also like

- [Assembly systems planning with use of databases and simulation](#)  
Š Vaclav, P Kostal, D Michal et al.
- [Study of the illite-kaolinite-CaCO<sub>3</sub> mixtures during firing](#)  
D Mikušová, T Hůlan, F Luká et al.
- [AC conductivity of C130 type electroporcelain as a function of firing temperature and compaction pressure](#)  
Š. Csáki, O. Al-Shantir, M. Vrabec et al.



**ECS**  
The  
Electrochemical  
Society  
Advancing solid state &  
electrochemical science & technology

**DISCOVER**  
how sustainability  
intersects with  
electrochemistry & solid  
state science research

# Analysis of the machine frame stiffness using numerical simulation

Š Vrtiel, Š Hajdu and M Behúlová

Slovak University of Technology in Bratislava, Faculty of Materials Science and Technology in Trnava, Ulica Jána Bottu č. 2781/25, 917 24 Trnava, Slovakia

stefan.vrtiel@stuba.sk

**Abstract.** The paper deals with the numerical modelling and simulation of loads arising during the milling process and their impact on the deformations and stresses developed in the frame of construction of hobby milling machine. Based on the prepared simulation model, the loads during the machining with feed rates in different directions were considered in order to find out the critical loading and its influence on the machine frame deformation. The impact of the frame deformations on the displacement of a tip of the tool, and thus the accuracy of the machining process was evaluated. Results of initial numerical simulations provided also the information about the components of the construction that need to be modified during the optimization of the designed construction and/or the development of a new prototype.

## 1. Introduction

Compared to the past, the advantages of numerical simulations are increasingly used in the design and development of machine components. While they were once applied mostly for the verification of real experiments, today they are used to the same extent in the phase of a product development [1, 2]. This is confirmed also by the integration of tools for numerical simulation directly to the current CAD systems such as Autodesk Inventor®, SolidWorks®, CREO® CATIA® [3-6] or new interface modules for engineers like ANSYS AIM [7].

Based on the results of numerical analyses and simulations, the new product can be optimized very efficiently. Consequently, duration of the development phase can be significantly shorter. Such a progressive approach to the development process contributes to the increase in competitiveness of an enterprise through the saving time and financial resources [8, 9]. Moreover, application of numerical testing and simulation provide the possibility to investigate several design virtual prototypes of the developed product including geometrical or material options and to evaluate their influence on product behaviour under different boundary conditions and/or loading and in some cases also to predict the efficiency and the product lifetime [10, 11]. These information and knowledge allow the designer to change the product design or even the product concept itself. In some cases, these procedures lead to the discovery of completely new technical solutions. Of course the final product design could not be realized without verification of simulation model and computed results on its physical prototype.

This paper presents the simulation model developed for the initial static stress-strain analysis of the construction frame of a designed hobby milling machine subjected to the different types of loading during a milling process. The main aim of numerical simulations is to evaluate the stiffness of the machine frame and to determine the critical loads causing the maximal deformations and stresses in order to reveal the weak points of construction design.



## 2. Problem description and calculation of a cutting force

The portal 3D milling machine (Figure 1) designed mainly for the hobby segment was subjected to the analysis. The design of the construction took into account the lowest weight of the machine [12] what is related to the load and the required power for the driving units. The basic dimensional characteristics of the machine are summarized in Table 1.

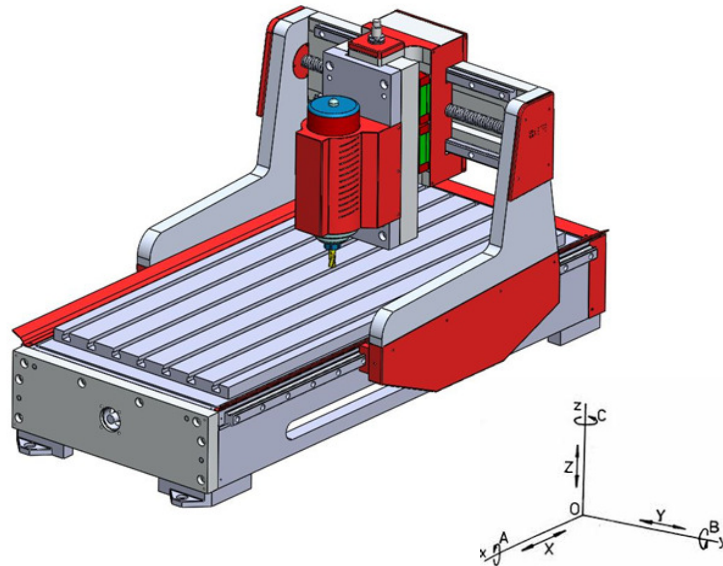


**Figure 1.** Design of a milling machine.

**Table 1.** Dimensional parameters of the milling machine.

Machine dimensions	Value	Units	Feed axes (travel)	Value	Units
Length	975	mm	X	500	mm
Width	539	mm	Y	300	mm
Height	563	mm	Z	120	mm

For the simulation, the milling process with a two flute centercutting milling tool was chosen. In this process, the maximum cross-sectional area of the layer to be removed and hence the maximum load is known on the base of the cutting depth  $a_p$ , the feed rate  $f_z$  and the cutting resistance of the machined material  $k_c$ . Considering the maximum cross-sectional area of the removed layer and other selected technological parameters presented in Table 2, the values of the cutting force components were determined using the relationships (2)-(4).

**Table 2.** Selected technological parameters.

Parameter	Nomenclature	Value	Units
Tool diameter	$D$	5	mm
Number of tool flute	$n_z$	2	-
Cutting depth	$a_p$	2	mm
Cutting width	$a_e$	5	mm
Cutting speed	$V_c$	300	m.min <sup>-1</sup>
Feed rate	$f_z$	0.1	mm.tooth <sup>-1</sup>
Angle of heel edge	$\lambda_s$	25	degree
Specific cutting resistance	$k_{cl}$	830	MPa

Calculation of the cutting resistance:

$$k_c = \frac{k_{c1}}{f_z^m} = \frac{830}{0.1^{0.23}} = 1409.54 \text{ MPa} \quad (1)$$

The exponent  $m$  denotes the slope of the linear dependence of  $k_{c1}$  on the chip thickness. Its values for various materials can be obtained on base of experiments [13].

Calculation of the main (tangential) cutting force  $F_c$ :

$$F_c = a_p f_z k_c K_\gamma K_{wear} = 2 \times 0.1 \times 1409.54 \times 0.86 \times 1.5 = 363.66 \text{ N} \quad (2)$$

where  $K_\gamma$  is the front angle correction parameter,  $K_{wear}$  is the correction parameter according to wear [13].

Calculation of radial cutting force  $F_{rad}$ :

$$F_{rad} = F_c k = 363.66 \times 0.7 = 254.56 \text{ N} \quad (3)$$

where  $k$  represents the ratio between radial and tangential cutting force.

Calculation of axial cutting force  $F_{ax}$ :

$$F_{ax} = 0.28 F_c \text{tg}(\lambda_s) = 0.28 \times 363.66 \times \text{tg}(25^\circ) = 47.48 \text{ N} \quad (4)$$

### 2.1. Analysis of stiffness in single motion modes

In Figure 2, the feed directions  $V_{f1}$ ,  $V_{f2}$  and  $V_{f3}$  are illustrated for the possible situations which can occur during milling with given technological conditions. The movement of the tool in the feed directions  $V_{f1}$  and  $V_{f2}$  is accomplished by moving of the entire machine portal. The  $V_{f3}$  feed movement is performed only by the support moving along the portal. Thus, the directions of cutting forces will vary together with the simulated feed direction.

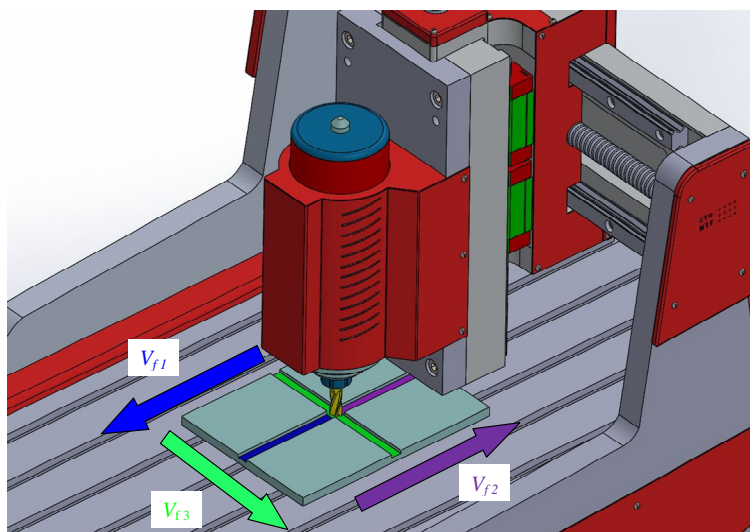


**Figure 2.** Illustration of possible feed directions  $V_{f1}$ ,  $V_{f2}$  and  $V_{f3}$ .

### 2.2. Simulation model

In order to evaluate the tool stiffness using numerical simulation, the simulation model was developed. The geometrical model was adjusted by the top-down method of modelling [8]. For calculation, the detailed input CAD model was simplified by removal or editing some technological elements which are supposed to have no significant influence on the results of numerical simulation. These changes were also necessary to make to generate appropriate finite-element mesh. Elements such small size threads (M5), small bumps for easier assembly and complex shape areas were removed or adapted. Editing the resulting assembly also consisted of removing the fasteners such as bolts and locking pins. Screws and locking pins were replaced by fixation bonds representing their functionality in the simulation model.

For more accurate results, the option "No Separation" was chosen for the optimal definition of contact on the adjacent areas. This contact description represents the real contact of two adjacent surfaces with the possibility to evaluate the surface pressure in the contact area. On the other hand, it does not remove the degrees of freedom relative to the adjacent component as e. g. the "Bonded" option that prevents them from the movement relative to each other like in the case of the spike contact region of the ball screw and the nut. Overall, thirty-nine contacts were defined in the simulation model.

### 2.3. Finite element mesh

The accuracy of numerical calculations depends significantly on the density and the quality of generated finite-element mesh. In this reason, remarkable attention was paid to the mesh generation and to its quality evaluation. The final finite-element mesh (Figure 3) contains the total number of 424 238 elements with the maximum element side length of 3 mm.

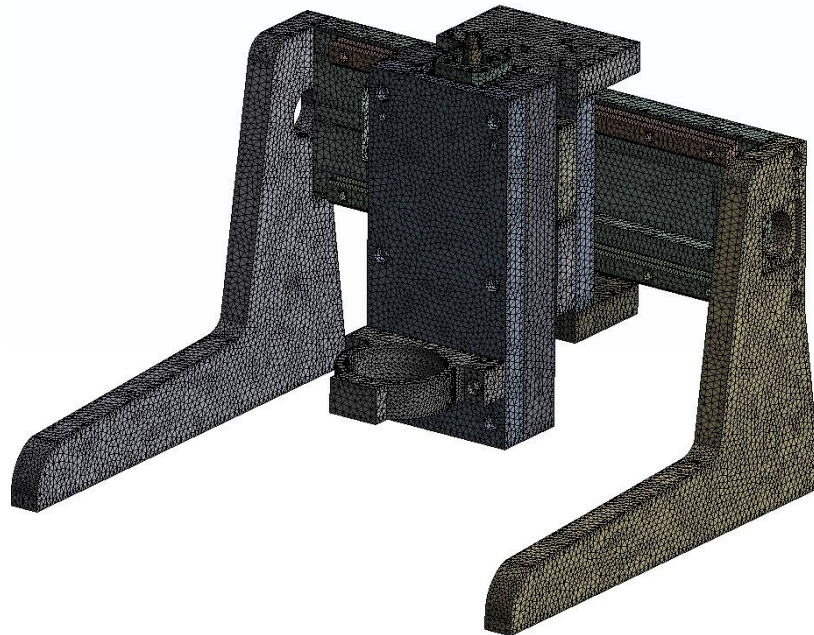


**Figure 3.** Model with generated finite element mesh.

### 2.4. Material model

The material model contains the properties of two materials, EN AW 7075 aluminium alloy and the EN S195T steel given in Table 3. The supporting part of the structure is supposed to be produced from the aluminium alloy, linear guides, ball screws and mounting screws are designed from the steel. Material properties from the database of ANSYS Workbench [14] were applied.

**Table 3.** Physical and mechanical properties of applied materials [14].

Property	Aluminium alloy	Structural steel	Units
Density	2770	7850	kg.m <sup>-3</sup>
Young modulus	71000	200000	MPa
Yield strength	280	250	MPa
Tensile strength	320	490	MPa

### 2.5. Loads and boundary conditions

The distribution of cutting forces varies according to the machining direction (Figure 4). The radial component  $F_{rad}$  of the cutting force  $F_c$  is particularly responsible for the change of loading direction as it is acting in the opposite direction to the feed direction during the machining. In addition to cutting forces, the gravitational force and force resulting from the weight of a virtual spindle with the value of  $F_v = 50$  N were included to the simulation model.

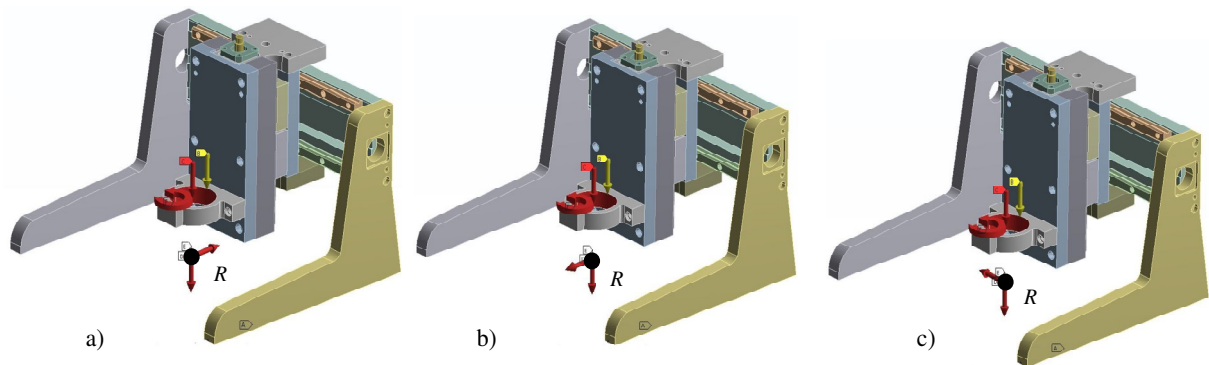


**Figure 4.** Schematic representation of acting loads in the direction of a) feed rate  $V_{f1}$ , b) feed rate  $V_{f2}$ , c) feed rate  $V_{f3}$ .

### 3. Results and discussion

The *Probe Deformation* was developed in the simulation model, to evaluate the effect of the structure deformation on the accuracy of the machining process under the specified load. This tool enables to measure the influence of the structure deformation on the displacement of a point created in the location of acting cutting force or in other words in the contact point of the milling tool and the workpiece. This point will be referred to as the point  $R$  (Figure 4).

The resulting deformations of the designed frame of construction caused by the machining with the feed rates of  $V_{f1}$ ,  $V_{f2}$  and  $V_{f3}$ , are illustrated in Figure 5, Figure 6 and Figure 7, respectively. The obtained results revealed a significant absence of stiffness, especially in the case of feed rate  $V_{f1}$  (Table 4).

**Table 4.** Computed displacements of due to the machining feed rate of  $V_{f1}$ ,  $V_{f2}$  and  $V_{f3}$ .

Result	Feed rate		
	$V_{f1}$	$V_{f2}$	$V_{f3}$
Displacement of a point $R$ in X-direction [mm]	-0.170	0.070	-0.048
Displacement of a point $R$ in Y-direction [mm]	-0.150	0.034	-0.056
Displacement of a point $R$ in Z-direction [mm]	$-3.17 \times 10^{-4}$	$2.67 \times 10^{-4}$	-0.060
Magnitude of the displacement of a point $R$ [mm]	0.228	$7.76 \times 10^{-4}$	0.095
Resulting deformation of the frame [mm]	0.230	0.075	0.103

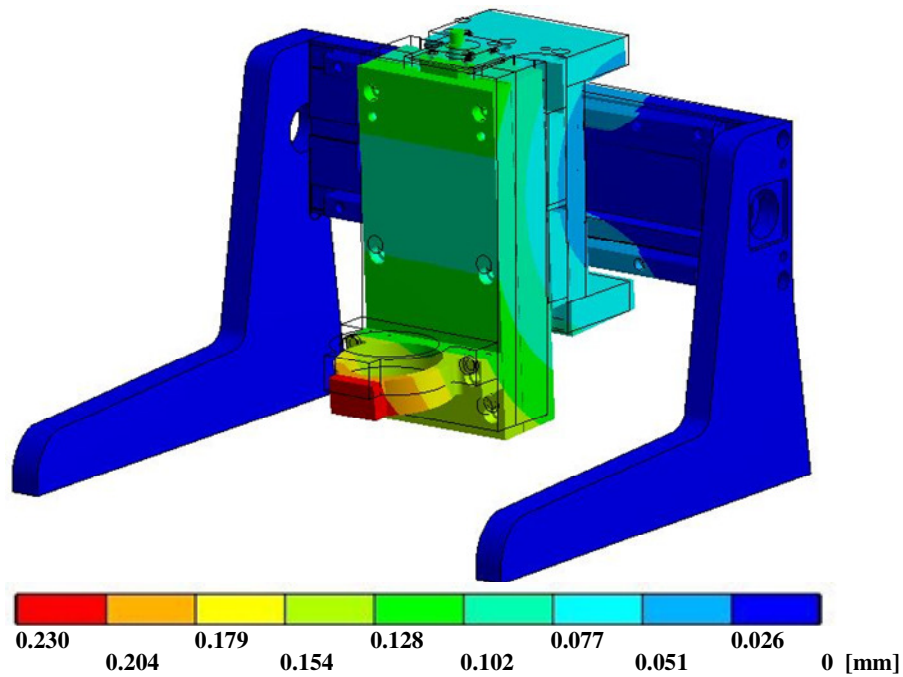


**Figure 5.** Deformation of the designed frame of construction caused by the machining with the feed rate  $V_{f1}$

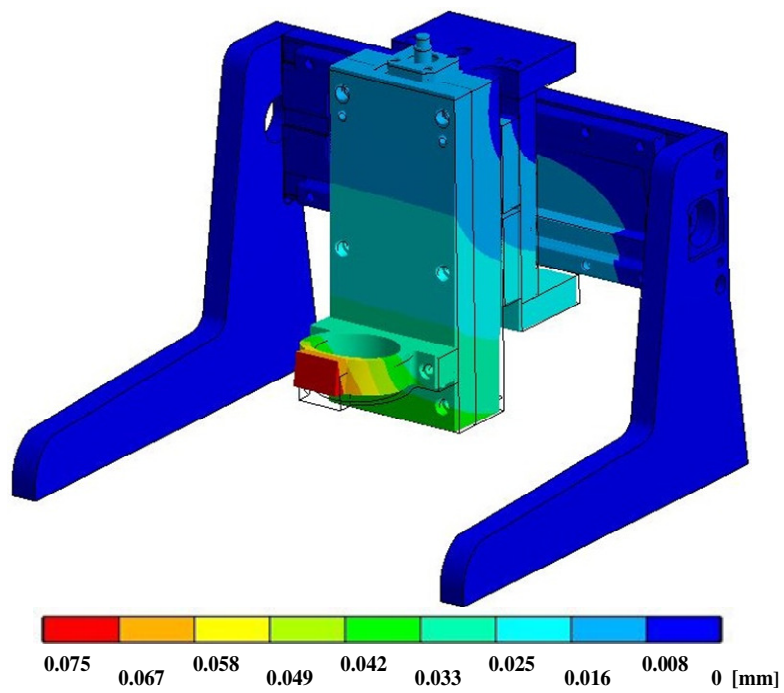


**Figure 6.** Deformation of the designed frame of construction caused by the machining with the feed rate  $V_{f2}$ .

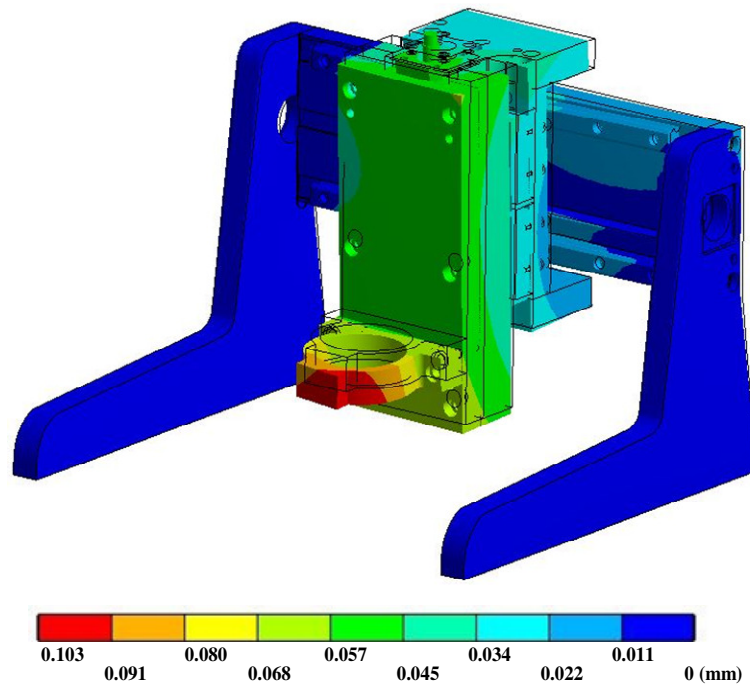


**Figure 7.** Deformation of the designed frame of construction caused by the machining with the feed rate  $V_{f3}$ .

The maximum deformation of the analyzed frame of construction was computed by the machining with the feed rate of  $V_{f1}$  at the level of 0.230 mm, while the displacement of the point  $R$  from its defined (ideal) position was 0.228 mm (Table 4). The deformations of the frame of construction resulting from the  $V_{f2}$  feed direction was the lowest. The maximum frame deformation in this case is 0.075 mm which is only 32% of the maximum value of deformation computed for the feed rate  $V_{f1}$ . The maximum deformation of the construction frame in the case of the feed rate  $V_{f3}$  was 0.103 mm representing 45% of the maximum deformation for the feed rate  $V_{f1}$ .

The highest value of von Mises stress at the level of 29.56 MPa was localized in the linear guides ( $Y$ -axis) and the spindle holder of the milling machine (Figures 8). The spindle holder is an important part of the machine tool construction. Results of numerical simulations indicate that the maximum stresses are concentrated right in this part. In this reason, the particular attention must be paid to this component when the design modification and changes will be accomplished.

Generally, proper changes and modifications of the geometry and/or materials applied for critical, the most loaded parts of milling machine would bring significant improvement of CNC machine stiffness. Aluminium alloys are used in the hobby segment in the largest range because of their good machinability and the low weight compared to steel (almost three times lower weight). The weight of the components is also determining for other properties and parameters of the machine. Moreover, the driving units with the less power can be used leading to the further reduction of the weight of the machine and its equipment. The optimal solution could be a hybrid construction consisting of combination of an aluminium alloy and steels that would be used for components subjected to higher loading. The modification of the supporting components can also be achieved by changing of the design using the ribbed components. Today, such design elements are often used in design of milling machines because the components with ribbed geometry generally better respond to static and dynamic loading [7].

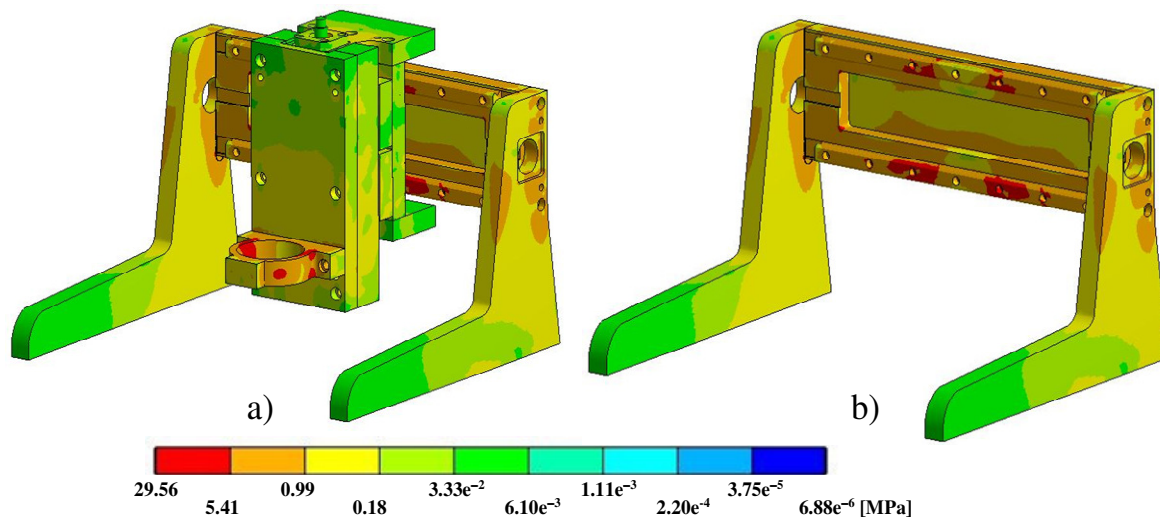


**Figure 8.** Distribution of von Mises stresses a) in the designed frame and b) in the linear guides due to the machining with the feed rate  $V_{fl}$ .

Based on the results of numerical simulations, not only the optimal shape of single components of a milling machine for the conditions in which the resulting product will be exploited can be designed but also the optimal geometric and shape arrangement of the functional elements of the product can be improved considering one or more selected parameters. The selected parameters can be for example the maximum performance, efficiency or the minimum price, weight, stresses, deformations, increase in service life or others. In the performed numerical simulation, the selected parameter was the deformation of the frame which further determined the machine accuracy.

#### 4. Conclusions

The paper deals with the modelling and numerical simulation of loads arising in the milling process and their impact on the deformations and stresses developed in the frame of construction of hobby milling machine. For the static stress-strain analysis of the machine frame subjected to the different types of loading during a milling process, the simulation model was developed and used for the evaluation of deformations and stresses during the machining with the feed rates in different directions. In addition to the deformation of the machine frame, the accuracy of the milling tool positioning represented by the displacement of the reference point  $R$  was investigated.

As it follows from the results of numerical simulations, the maximum deformation of the machine frame at the level of 0.230 mm was attained for the machining with the feed rate  $V_{fl}$  in the direction of  $X$ -axis. The highest value of von Mises stress of 29.56 MPa was localized in the linear guides and the spindle holder of the milling machine. The displacement of the tip of milling tool in the reference point  $R$  from its defined position was 0.228 mm. It must be noted that in the direction of  $X$ -axis the machine has the maximum feed axis travel of 500 mm. The positioning of larger workpieces is assumed to be accomplished in such a way that the machine feed rate in this axis is exploited the most. From this point of view, it is necessary to revise the design of the machine with the particular attention on the machine stiffness in the direction of  $X$ -axis.

#### Acknowledgments

Research has been supported by the Programs to support excellent young researchers and research teams (EBW-AHSS 1387 and 1347/PRO-MAT-ZVAR) of STU Bratislava.

## References

- [1] Gajdoš J 2015 *The Future of CAD Systems CAD* **5**
- [2] Marijn P, Zwier W and Wits W 2017 Physics in Design: Real-time Numerical Simulation Integrated into the CAD Environment *Procedia CIRP* **60** 98-103
- [3] Autodesk Inc. San Rafael California USA
- [4] SolidWorks SIMULATION Dassault Systèmes Vélizy-Villacoublay France
- [5] Creo Simulate PTC - Parametric Technology Corporation, Needham, Massachusetts, USA.
- [6] CATIA Dassault Systèmes Vélizy-Villacoublay France
- [7] Hloužek J 2015 *ANSYS AIM- Physically linked analyzes in one program environment CAD* **5**
- [8] Marek J 2014 *Construction of CNC machine tools 3* (Prague: MM publishing)
- [9] Hong C C 2016 Static structural analysis of great five-axis turning–milling complex CNC machine *Engineering Science and Technology* **19** 1971-1984
- [10] Liangchao Z, Ming L and Ralph R M 2016 *Direct simulation for CAD models undergoing parametric modifications* *Computer-Aided Design* **78** 3-13
- [11] Łukaszewicz K 2017 Use of CAD Software in the Process of Virtual Prototyping of Machinery *Procedia Engineering Journal* **182** 425- 433
- [12] Möhring H, Brecher C and Abele E 2015 Materials in machine tool structure *CIRP Annals – Manufacturing technology* **64** 725-748
- [13] Rejt M and Píška M 2006 *Teorie obrábění, tváření a nástroje* (BRNO: Akademické nakladatelství CERM) **1** 225
- [14] ANSYS Inc. Computer software Pennsylvania, United States